On-line optimization of dual-fuel combustion operation by extremum seeking techniques

Author, co-author (Do NOT enter this information. It will be pulled from participant tab in MyTechZone)

Affiliation (Do NOT enter this information. It will be pulled from participant tab in MyTechZone)

Abstract

Dual-fuel combustion engines have shown the potential to extend the operating range of Homogeneous Charge Compression Ignition (HCCI) by using several combustion modes, e.g. Reactivity Controlled Compression Ignition (RCCI) at low/medium load, and Partially Premixed Compression Ignition (PCCI) at high load. In order to optimize the combustion mode operation, the respective sensitivity to the control inputs must be addressed. To this end, in this work the extremum seeking algorithm has been investigated. By definition, this technique allows to detect the control input authority over the system by perturbing its value by a known periodic signal. By analyzing the system response and calculating its gradient, the control input can be adjusted to reach optimal operation. This method has been applied to a dual-fuel engine under fully, highly and partially premixed conditions where the feedback information was provided by in-cylinder pressure and NO_x sensors. The gasoline fraction and the injection timing were selected as control inputs and an extremum seeking controller was designed and verified to optimize brake efficiency by tracking the ideal combustion phasing and to reduce NO_x emissions as well.

Introduction

The internal combustion engine (ICE) industry is facing substantial challenges in order to comply with the urgent need for cleaner transportation technologies. Throughout the years, the research community investigated less polluting combustion concepts which are part of the so called low temperature combustion (LTC) category [1,2]. These combustion strategies aim to emit less nitrogen oxides (NO_x) and soot while maintaining high brake thermal efficiencies. Among the various concepts, dual-fuel combustion such as Reactivity Controlled Compression Ignition (RCCI) exhibits a great potential to address the pollutant emissions issue as well as the control authority obstacle encountered in Homogeneous Charge Compression Ignition (HCCI) strategy [3–5]. This approach consists in injecting two fuels of different reactivities, e.g. gasoline and diesel, and by regulating their blending ratio the mixture reactivity can be controlled and therefore allows to trigger the combustion [6]. The low reactivity fuel is commonly injected in the cylinder with port fuel injectors (PFI) during the intake stroke, and the high reactivity fuel is injected directly into the cylinder with direct injectors (DI) allowing multiple injections and various injection scenario.

Dual-fuel combustion might be found in various injection strategies with different levels of mixture stratification. When the high reactivity fuel is injected far before the top dead center, the mixture is close to homogeneous conditions and the combustion is therefore kinetically controlled, i.e. the RCCI concept. In these conditions, low combustion temperature is achieved and high exhaust gas recirculation (EGR) rates allow to reduce significantly the NO_x emissions [7]. Nevertheless, the resulting high pressure rise rates limit the load operation and other dual-fuel strategies such as the Dual-Mode Dual-Fuel were therefore investigated and proposed [8,9]. In this strategy, when the load is increased and harmful conditions are reached due to the highly premixed charge, a single direct injection is moved into the top dead center vicinity reducing the mixing time and resulting therefore in a less reactive combustion. The side effect of this combustion mode is that, due to late injection, some diffusive-like combustion behavior might occur which results in an increase of the NO_x emissions.

A lot of effort was recently made towards NO_x reduction. Alongside to the LTC strategies, NO_x emissions can also be reduced in the exhaust tail pipe thanks to after-treatment systems such as lean NO_x traps (LNT) and selective catalytic reduction (SCR) [10,11]. Their efficient operation relies on a proper diagnostic which includes lambda (λ) and NO_x measurement and models [12,13]. NO_x sensors are getting higher attention and are being installed more often in commercial applications. This information is therefore interesting to enhance feedback strategies by considering the pollutant emissions into the control system.

Conventional combustion feedback controllers traditionally rely on in-cylinder pressure measurement [14–16]. While this strategy is efficient to maintain the engine performance against external disturbances, it fails to ensure optimal operation of the engine. Indeed, traditional engine test bench calibration prior to on-road application is performed in a controlled environment where a combustion phasing reference might be chosen for best efficiency and pollutant emissions trade-off. Nevertheless, in a real-use situation, if these conditions deviate from the expected ones the calibrated combustion phasing setpoint might no longer be optimal and its closed-loop control could therefore results in a worsened combustion operation. An efficient way to optimize the engine operation on-line is by means of extremum seeking technique. Extremum seeking (ES) is a model-free strategy that finds the input that minimizes/maximizes a function. By perturbing the system with a known periodic input signal and by analyzing the output response, the corresponding gradient can be obtained and therefore be used to seek for the extreme (i.e. optimal) region. This approach was introduced in

the 1920s [17] and has been since then investigated in many areas [18–20].

Gradient based algorithms such as extremum seeking were used in spark ignition engines to optimize the engine efficiency by controlling the spark advance timing [21–23]. Lewander et al. [24] applied an extremum seeking controller to a diesel engine where an optimal combustion phasing reference was evaluated and tracked to provide the best indicated efficiency. Van der Weijst et al. in [25] considered an ES controller for on-line fuel efficiency optimization in a diesel engine by adjusting the combustion phasing and pumping losses references to track minimum cost. Both air and fuel-path were considered and a NO_x sensor placed at the engine exhaust was used to constrain the control actions. Due to the sensor delay observed in NO_x sensors, Tan et al. [26] proposed to include the nitrogen oxides emissions in the cost function to be optimized by taking advantage of their correlation with the combustion temperature. By estimating the maximum in-cylinder temperature, the ES controller aimed therefore to reduce such value in order to reduce NO_x emissions.

In this work, an on-line optimization algorithm for a gasoline-diesel combustion engine is investigated. In particular, the extremum seeking method was chosen to minimize a cost function composed of optimal combustion phasing tracking and NO_x emissions reduction. The gasoline fraction and the main diesel injection timing were selected as control inputs and a controller was designed according to a frequency analysis of the combustion sensitivity under three combustion modes: fully, highly and partially premixed. Nitrogen oxides emissions optimization was made possible thanks to a smart NO_x sensor which was characterized to consider sensor measurement delay. The strategy was applied to dual-fuel highly premixed conditions where a significant reduction in emissions was appreciated while maintaining an acceptable brake fuel consumption level.

This article is organized as follows: next section presents the experimental setup used in this study with the engine and acquisition and control facilities. The third section formulates the optimization problem and the considered control system. In the fourth section, experimental data from three combustion modes are analyzed to evaluate the combustion sensitivity to different control inputs and an extremum seeking controller is designed accordingly. The on-line optimization solution is applied to a dual-fuel case and the results are presented in the fifth section. Finally, the last section highlights the contribution of this paper.

Experimental facilities

The experimental activities in this study were carried out with a six cylinder heavy-duty diesel engine (see specifications in Table 1) modified to run in dual-fuel combustion, i.e. each cylinder was equipped with a port fuel injector.

Table 1. Engine specifications

Bore x Stroke	110 mm x 135 mm
Connecting-rod length	212.5 mm
Compression ratio	12.2:1
Number of cylinders	6
Total displacement	7700 cm3

Commercial gasoline and diesel were used as low and high reactivity fuels respectively. The diesel was direct injected at a rail pressure P_{rail}, controlled by the commercial ECU, while the gasoline was port fuel injected at a constant injection pressure of 7 bar.

The control of the injection settings at each cylinder, i.e. duration of injection (DOI) and start of injection (SOI), was made possible by dedicated devices connected to an embedded Field Programmable Gate Array (FPGA) chassis from National Instruments (NI 9155). A NI 9752 module was used for cam and crank angle synchronization and the injectors pulses were generated by two NI 9751 and two NI 9758 modules for the direct and the port fuel injection, respectively. Specific injector look-up tables were used to convert the required fuel mass to the corresponding injection duration at each injection system.

The engine setup included a variable geometry turbine (VGT) controlled by the ECU for varying the boost pressure, and a high pressure (HP) exhaust gases recirculation valve to provide the desired air dilution which was controlled by CAN using a PXI-8512 card.

Each cylinder was equipped with an in-cylinder Kistler 6125C pressure sensor (P_{cyl}) and the intake pressure (P_{int}) was measured by a Kistler 4045A10 sensor. Both signals were monitored with a sampling frequency function of the engine speed using a research encoder set with a resolution of 0.2 crank angle degree (CAD) per sample. Additionally, a smart NO_x sensor was placed at the turbine outlet allowing to measure both lambda (λ) and NO_x concentration levels. The acquisition of the different signals was handled by a 16 analog channels acquisition card (PXIe-6358) connected to the real-time controller (PXIe-8135) from National Instruments which was in charge of processing and saving the data. A scheme of the engine control setup is shown in Figure 1 where the blue and gray arrows show the control and the acquisition flow respectively.

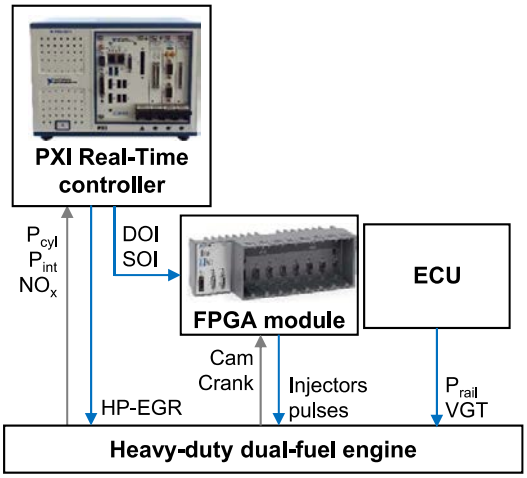

Figure 1. Experimental facilities layout: control actions (blue) and data acquisition (gray)

The in-cylinder pressure *pegging* [27] was done using the intake manifold pressure near the intake bottom dead center (BDC) and the combustion metrics, such as the crank angle where 50% of the combustion energy has been released (CA50), were obtained after filtering the in-cylinder pressure with a low-pass filter tuned at 2.5 kHz.

Problem formulation

The overall objective of this article is to propose and verify an on-line optimization algorithm for dual-fuel engine operation. To this end, it is necessary to define the quantity to optimize and which control inputs can operate the system to do so.

Optimization problem

The combustion phasing is a commonly adopted variable to track the highest engine brake efficiency. However, a trade-off exists between fuel consumption (i.e. brake efficiency) optimization and pollutant emissions reduction. In this work, it was therefore decided to include the NO_x sensor measurement into the function to consider the pollutant emissions optimization as well. The performance function resulted in the following cost function J which is to minimize:

$$J = \alpha\left|CA50 - CA50_{ref}\right| + \beta NO_x \tag{1}$$

where the first part aims to operate the engine in an efficient area provided by a previously calibrated value of $CA50_{ref}$, and the last part corresponds to the pollutant emissions criteria. The weighting factors α and β are used to emphasize the importance of each parameter in the final cost evaluation. When $\beta > 0$ the optimizer algorithm will attempt to reduce the NO_x level at the expense of an ideally phased combustion.

Control system

Both air and fuel-path are candidates to drive the engine operation to its minimum cost function area. Nevertheless, due to the slow dynamics at the air-path it was decided to focus the present work only on the use of the injection settings to handle the on-line optimization. Considering a dual-fuel combustion engine in constant load operation, two main control variables can be mentioned, the gasoline fraction and the direct injection timing:

- The gasoline fraction (GF) represents the mixture reactivity and is calculated as follows:

$$GF = \frac{m_g}{m_g + m_d} \tag{2}$$

  where m_g and m_d are the injected gasoline and diesel masses respectively. This quantity was found to delay the combustion as its value increases which is justified by the difference in resistance to auto-ignition between gasoline and diesel.

- The injection timing, or start of injection (SOI), of the direct injection drives the mixture stratification. At early timings, the mixture is close to homogeneous conditions, and when delayed, richer equivalence ratio distribution in the cylinder appears which add some control authority over the combustion evolution.

The NO_x emissions are sensitive to the combustion temperature, hence function of the combustion evolution where conditions near the TDC might raise their amount.

According to their influence on the combustion behavior, these two control variables were therefore considered as potential inputs for the present control problem.

Extremum seeking controller

In this work, the extremum seeking technique was chosen to optimize the engine operation according to the cost function J in (1).

Extremum seeking principle

The main advantage of the extremum seeking method is that it does not require a model of the system. Instead, it consists in perturbing the system control input with a given frequency around its original level and to seek for the optimum value by measuring the output response gradient. The system output signal might be connected directly to the extremum seeking controller or previously reordered in the form of an objective, or cost, function as it is in the present work. This signal is first band-pass (BP) filtered to remove the low frequency content, associated to the mean amplitude, and the high frequency content, associated to noise, to capture the objective function response to the input perturbation. The gradient is then estimated by multiplying the filtered signal by the perturbation, and the final correction to apply is obtained by integrating this value and by multiplying it by a calibrated gain. In order to evaluate the gradient, it is important to ensure that both the perturbation and the output of the BP filter signals are in phase. Indeed, in the case of sensor measurement delay for instance, while the perturbation would be incremented at the instant t_0, the sensor might provide the corresponding system response only at $t_{0+\Delta t}$, which can result in an incorrect gradient estimation and lead to unstable operation [26]. If necessary, the perturbation might therefore be shifted to comply with such requirement. The global extremum seeking principle architecture is shown in Figure 2 where the ES controller is delimited by a black dashed line. The gray dashed line encompasses the gradient and integration component of the extremum seeking controller. This section will be used later in this study due to the multi-variable architecture presented in this work. More information about extremum seeking algorithm can be found in [28,29].

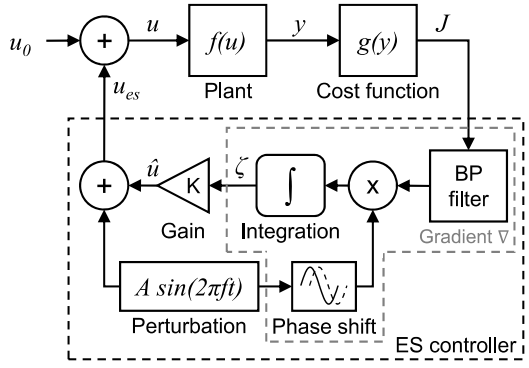

Figure 2. Conventional extremum seeking controller architecture for a single variable. A periodic perturbation of amplitude *A* and frequency *f* is applied to the original steady state input u_0. The plant output *y* is restructured into a cost function J which serves as an input to the extremum seeking (ES) controller. BP stands for *band-pass* filter.

Combustion sensitivity to control inputs

In order to design the extremum seeking controller for the considered system, i.e. the heavy-duty dual-fuel engine, it is necessary to analyze the system output response to the input perturbation. The perturbation frequency should be high enough to ensure a fast convergence to the optimal operation, but slow enough to properly observe the system response as well. Similarly, a high perturbation amplitude would promote optimization time reduction and ease the oscillation detection, but would result in a too excessive variation over the optimal point at the end of the process as well. Solutions were proposed to improve conventional extremum seeking architecture such as decreasing the perturbation amplitude as the system is getting closer to the optimal value [30], but such methods were not evaluated here.

Dual-fuel combustion can be found with different injection strategies depending on the operating conditions, namely: fully, highly and partially premixed. Each of these combustion modes is traditionally function of the engine load. At low load, highly premixed conditions is used to ensure enough mixture stratification and provide a well phased combustion. By increasing the load, more energy is available and the diesel injections can be advanced to reach fully premixed conditions ensuring low NO_x and soot emissions. Finally, at high loads the rapid auto-ignition of the mixture becomes critical and only partially premixed combustion can be safely achieved where a single diesel injection is moved in the vicinity of the top dead center. In these conditions the combustion might show some diffusive-like behavior, which penalizes the total NO_x emissions but extends the operating range of the dual-fuel combustion. Each combustion mode might therefore be more sensitive to a specific control variable depending on the operating conditions, e.g. a slight variation in the injection timing is expected to be less effective in the fully premixed case due to the higher mixture homogeneity.

In the previous section, $CA50$ and NO_x were selected to create the cost function to be optimized in (1), and GF and SOI were considered as possible control variables. The engine was therefore exposed to a perturbation applied to the gasoline fraction and the injection timing in the form of a chirp signal, respectively being *up-chirp* and *down-chirp*, in the three aforementioned combustion modes. The minimum and maximum frequencies applied were 0.05 and 0.6 Hz respectively, and the chosen amplitudes were 0.02 for GF and 1.5 CAD for SOI. An example is shown in Figure 3. The combustion phasing and the NO_x measurement were analyzed in the frequency domain and the results can be found in Figure 4. Table 2 presents the original conditions and settings of the experimental data and Table 3 summarizes the chirp signal calibration applied to obtain the results in this figure. Note that in Table 2, IMEP refers to the indicated mean effective pressure, SOI_p to the SOI of the pilot injection and SOI to the main injection timing. In this work, only the use of the main injection was evaluated in the extremum seeking design, i.e. the pilot injection timing was kept constant. Injection timings are expressed in CAD before top dead center (bTDC) while the $CA50$ indicates the crank angle after TDC (aTDC).

Table 2. Operating conditions of the experimental data used in the combustion sensitivity analysis (Figure 4)

Operating conditions		Fully premixed	Highly premixed	Partially premixed
Speed	[rpm]	1800	1800	1800
IMEP	[bar]	11.3	11.9	11.8
EGR	[%]	40	33	34
SOI_p	[°bTDC]	60	35	None
GF_0	[-]	0.73	0.66	0.60
SOI_0	[°bTDC]	46	15	13

Table 3. Chirp signal specifications applied on GF and SOI at various combustion modes

Chirp signal		GF	SOI
Amplitude A	[-]/[CAD]	0.02	1.5
Frequency f	[Hz]	From 0.05 to 0.6	From 0.6 to 0.05

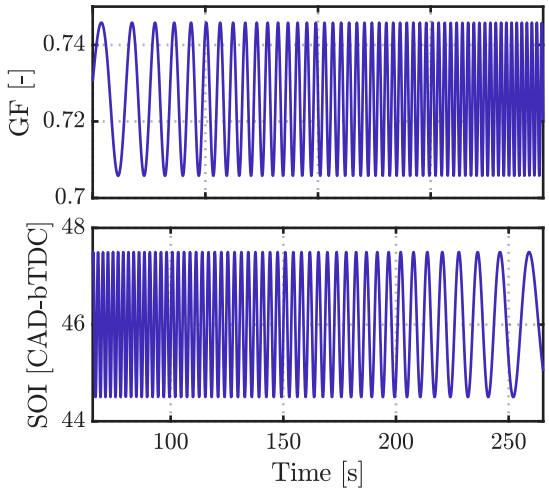

Figure 3. Chirp perturbation in GF (top) and SOI (bottom). Details can be found in Table 2 and Table 3.

For illustration purposes, in Figure 4, the top plots show the in-cylinder pressure p_{cyl}, the heat release rate dQ and the direct diesel injector signal of a typical cycle at each combustion mode to appreciate the operating conditions. Here the gasoline injection signal is not shown because its timing was at the same moment for the three combustion modes, i.e. during the intake stroke. According to the notation used in Figure 2, the starting control variable u_0 consisted in GF_0 and SOI_0 and these quantities were varied by a perturbation of amplitude A and frequency f as stated in Table 3. Note that the extremum seeking controller is not active in this case and therefore $\hat{u}$ is equal to zero. Middle and bottom plots show respectively the short-time Fourier transform (STFT) of the $CA50$ and NO_x signals. As expected, it can be seen that the gasoline fraction is the dominant control variable in fully premixed conditions because of the kinetically controlled combustion, while the injection timing takes the advantage in partially premixed combustion. Highly premixed condition represents an in-between

configuration where both of the control variables have some authority over the combustion. These conclusions are especially true for the $CA50$ response. In the case of the NO_x signal, it is observed that the highest response magnitude tends to be in the range of frequencies under 0.3 Hz. More importantly, this figure shows that both $CA50$ and NO_x respond to a perturbation in GF and SOI, verifying therefore that the extremum seeking controller should be able to find the optimal cost function area thanks to these two control variables no matter the combustion mode operation.

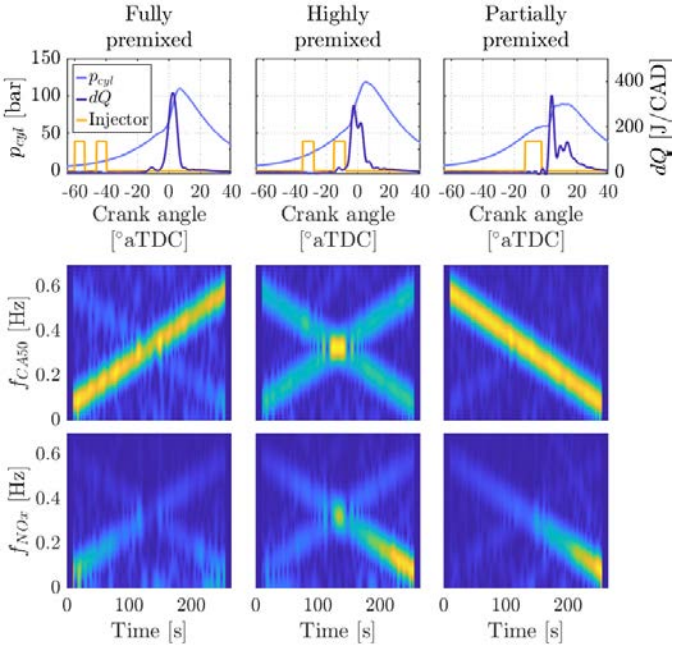

Figure 4. $CA50$ and NO_x response to chirp perturbation in GF and SOI at various combustion modes. Details can be found in Table 2 and Table 3. Top plots: in-cylinder pressure p_{cyl}, heat release rate dQ and direct injector signal. Middle plots: STFT of the $CA50$ signal. Bottom plots: STFT of the NO_x signal

Dual-fuel extremum seeking controller

In the present study, the cost function J in (1) is composed of two distinct parts, $CA50$ and NO_x. Consequently, each part should be processed by the extremum seeking controller to calculate their contribution to the final correction. The ES controller shown in Figure 2 was therefore modified to integrate the multiple input architecture. Figure 5 shows the structure of the redesigned ES controller where the gradient section in gray is detailed in Figure 2, and J_1 and J_2 are the components of the total cost function, that is in this case:

$$J_1 = J_{CA50} = \alpha\left|CA50 - CA50_{ref}\right| \tag{3}$$

$$J_2 = J_{NO_x} = \beta NO_x \tag{4}$$

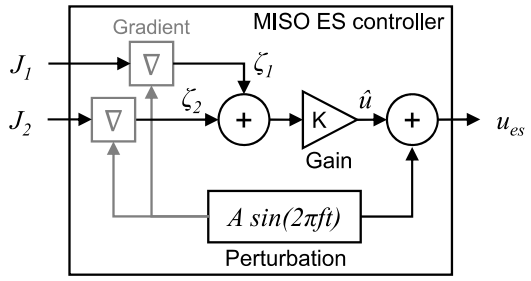

Figure 5. Multi-input single-output (MISO) extremum seeking controller scheme

The NO_x measurement is subject to sensor and gas transport delay. Consequently, as it was previously mentioned, the sensor needs to be characterized in order to include its phase shift in the extremum seeking controller to obtain the corresponding gradient and avoid unstable execution. One method consists in performing an input step and deriving the dynamics with a linear first order model [31]. Here, it was decided to identify the NO_x dynamics by perturbing the injection timing in order to evaluate the response to be expected in the investigated application. To this end, partially premixed conditions were chosen to accentuate the injection timing effect on the NO_x emissions. First, a simple linear static model was obtained by measuring the NO_x levels as a function of the injection timing around the considered operating point. Then, the NO_x measurement was believed to follow a first order filter behavior with a dead time τ (sensor delay) as follows:

$$NO_x(t) = \gamma NO_x(t - \delta t) + (1 - \gamma) NO_x^{model}(t - \tau) \tag{5}$$

where δt is the time step between two measurements, NO_x^{model} is the output of the aforementioned linear model and γ the filter calibration constant. The perturbation frequency at the injection timing was linearly increased and a least mean squares fitting between the measurement and the filtered signal provided the following calibration constants: $\gamma = 0.96$ and $\tau = 1\ s$, where the response time agreed with what can be found in the literature. The resulting signals can be seen in the bottom plot of Figure 6 where the static model is phased with the injection timing in the top plot. It can be observed that by increasing the frequency, the sensor is not only characterized by its dead time, but the magnitude is decreased as well because not enough time is available to measure the real emissions. This statement agrees with the conclusions from Figure 4 where the highest magnitudes in the NO_x measurement response were observed at low frequencies.

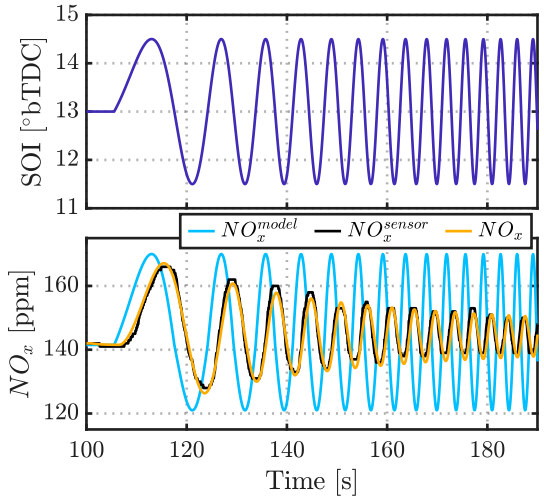

Figure 6. NO_x sensor characterization: injection timing as the control input (top) and resulting NO_x emissions (bottom)

The final design of the extremum seeking control application used in this work in shown in Figure 7 where each ES controller includes the architecture shown in Figure 5. This controller was applied to the heavy-duty engine presented in the second section and the results are detailed in the following section.

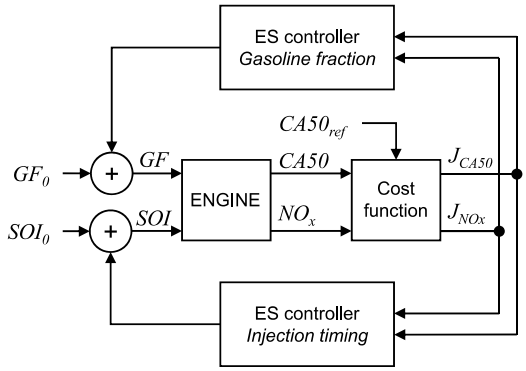

Figure 7. Dual-fuel extremum seeking controller structure

Results and discussion

The extremum seeking controller described in the previous section was applied to dual-fuel operation where highly premixed conditions were selected for its validation, see Table 4. These conditions were selected because they represent an in-between operation (compared to fully and partially premixed) where both GF and SOI should be driving the combustion to its optimal operation area. The controller settings are listed in Table 5 and the results are illustrated in Figure 8. In these results, the perturbation for J_{NO_x} was shifted by a constant $\tau = 1\ s$, while it remained unshifted for J_{CA50} due to the cycle-by-cycle evolution of the combustion phasing with respect to a change in the control input. Note that the eventual delay generated by the port fuel injection dynamics (wall wetting effect) [32] were considered insignificant according to the slow frequency chosen for the gasoline fraction perturbation.

Two conditions are shown in this figure: (i) in the first part, the ES controller is evaluated with the following cost function calibration: $\alpha = 1$, $\beta = 0.1$ and $CA50_{ref} = 4$ CAD-aTDC. And finally (ii), the area colored in gray shows the system response when β was modified from 0.1 to 0. The objective of the present validation is to evaluate the controller ability in dual-fuel conditions to respond to the cost function definition and calibration using the gasoline fraction and the injection timing as control inputs. By removing the NO_x weight from the cost function, the controller is expected to track the combustion phasing reference and leave the NO_x emissions free of any control action.

Table 4. Operating conditions of the experimental data used for the extremum seeking controller validation

Speed	[rpm]	1800
IMEP	[bar]	10.3
EGR	[%]	35
SOI_p	[°bTDC]	60
GF_0	[-]	0.735
SOI_0	[°bTDC]	22

Table 5. Extremum seeking controller settings for dual-fuel operation validation in highly premixed conditions

		GF	SOI
A	[-]/[CAD]	0.01	1.5
f	[Hz]	0.05	0.2
$f_{bandpass}^{cutoff}$	[Hz]	[0.02 - 0.1]	[0.1 - 0.4]
K	[-]	-0.05	-0.1

In Figure 8, $CA50_{ref}$ is shown with a black dashed line. It can be observed that although its value was set to 4 CAD-aTDC, the controller ended in a delayed combustion phasing, around 7 CAD-aTDC, when $\beta > 0$. This is due to the parallel NO_x optimization where the controller seeks to decrease the nitrogen oxides emissions at the expense of the combustion phasing. The combustion was therefore further delayed, which resulted in less in-cylinder pressure and temperature and consequently NO_x emissions. Note that due to the actual definition of J in (1) and the original levels of NOx in these conditions, even a small β value represents a significant weight amount in the cost function evaluation.

At the beginning of the test it is observed that $CA50$ and NO_x signals are made of two distinct frequency components (corresponding to GF and SOI actions), whereas after 150 seconds, GF seems to become predominant. Increasing the gasoline fraction not only delays the combustion and decreases the NO_x emissions, but it increases the homogeneous proportion of the mixture as well. Consequently, the simultaneous advance in the direct injection bringing further the mixture to higher premixed conditions, this is thought to result in a greater gasoline fraction effect over the combustion.

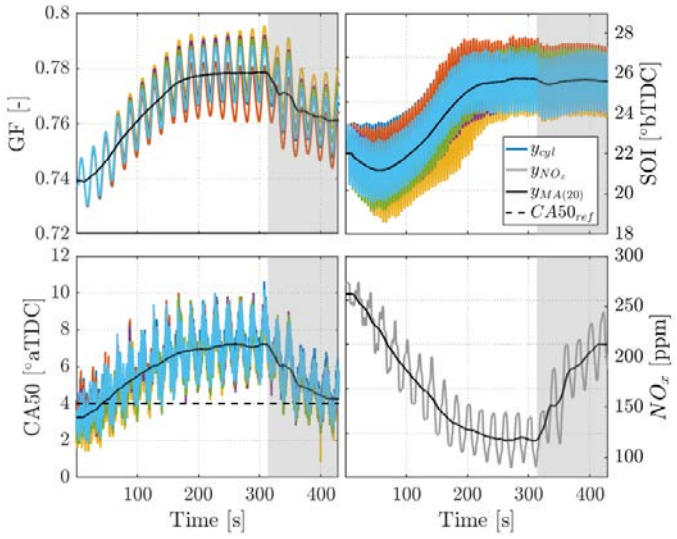

Figure 8. Dual-fuel extremum seeking controller results in highly premixed conditions. Each color represents a cylinder and the gray color is used for NO_x. The moving average (MA) over 20 seconds is represented in black and the notation *y* stands for the signal representation of the variable on the y-axis in each plot. The gray colored area on the right part shows the results when NO_x emissions are taken out of the optimization problem.

According to the levels shown by the moving average over 20 seconds in a continuous black line, in the first part of the test the gasoline fraction was increased from 0.735 to 0.78 and the injection timing was advanced from 22 to 25 CAD-bTDC. This resulted in a delayed combustion exhibited by the $CA50$ moving from 3.2 to 7 CAD-aTDC. In particular, the final GF and SOI corrections were aimed at NO_x optimization while maintaining a certain control authority over the required $CA50$ level, i.e. 4 CAD-aTDC. Note that in dual-fuel combustion, a gasoline fraction limitation should be considered in order to avoid unstable combustion operation where very high concentration might lead to misfire conditions due to low mixture reactivity and late combustion.

As previously mentioned, the combustion phasing is traditionally used to track the best brake efficiency. In this case, the combustion phasing was not driven to the desired level which resulted in an increase in the brake specific fuel consumption (BSFC) of 4%. Nevertheless, a 54% reduction in the brake specific NO_x (BSNOx) was measured thanks to the extremum seeking control actions. A trade-off between fuel efficiency and pollutant emissions exists and one can set the priority to the desired feature by tuning the cost function. Finally, it must be noticed that the cylinder-to-cylinder dispersion in the $CA50$ was also reduced thanks to the use of the ES controller which resulted in a standard deviation σ of 0.40 CAD compared to 0.65 at the beginning of the test (see Table 6).

Table 6. Extremum seeking outcomes at the start and at the end of the execution with $CA50$ and NO_x optimization, first part of the validation test

		Start	End (~300s)	Relative difference
σ_{CA50}	[CAD]	0.65	0.40	-38%
BSFC	[g/kWh]	202	210	4%
BSNOx	[g/kWh]	2	0.92	-54%

In the last part of the test (i.e. gray area) the weighting factor β was set to 0 and it can be observed that the $CA50$ is therefore driven to the combustion phasing reference which resulted in a NO_x emissions increase. Note that the gasoline fraction remains the principal control input in this case. This is thought to be justified by the further highly premixed conditions attained at the end of the first part where the injection timing was found to already have less influence.

It is important to note that an improved definition of the cost function with further calibration effort should result in a case where the combustion phasing can be moved to its reference while maintaining the NO_x emissions to the lowest level. This is considered as a potential future work where additional constraint features could be included in the control system design as well.

Summary and conclusions

This work investigated an optimization tool adapted to a dual-fuel combustion engine running with gasoline and diesel. In particular, a cost function has been specified which included tracking of a calibrated $CA50$ reference setpoint for high brake efficiency and minimum NO_x emissions. Extremum seeking was selected for its model-free aspect and its capacity to optimize a system operation by tracking the local minimum of the cost function.

Two control variables were chosen to design the extremum seeking controller: the gasoline fraction and the main injection timing. In the first place, these variables were subjected to a perturbation following a chirp signal to observe the system response under three combustion modes: fully, highly and partially premixed. The short-time Fourier transform of $CA50$ and NO_x were studied and it was found that the gasoline fraction GF had the highest control authority in fully premixed conditions, while the opposite was true in partially premixed where the injection timing was dominant. The combustion phasing was found to be sensitive along the complete frequency range while the NO_x exhibited a higher sensitivity to low frequencies.

The designed extremum seeking controller was applied to a highly premixed dual-fuel combustion case and the results showed that this strategy was able to improve the combustion operation by reducing the NO_x emissions by 54%, although at the expense of a 4% increase in the BSFC. These data show the potential of this technique to achieve optimal operation in such systems where the cost function can be enhanced by additional measurements and calibration.

References

[1] M. Alriksson, I. Denbratt, Low Temperature Combustion in a Heavy Duty Diesel Engine Using High Levels of EGR, SAE Tech. Pap. 2006 (2006) 75–2006. http://dx.doi.org/10.4271/2006-01-0075.

[2] A.K. Agarwal, A.P. Singh, R.K. Maurya, Evolution, challenges and path forward for low temperature combustion engines, Prog. Energy Combust. Sci. 61 (2017) 1–56. https://doi.org/10.1016/j.pecs.2017.02.001.

[3] S.L. Kokjohn, R.M. Hanson, D.A. Splitter, R.D. Reitz, Fuel reactivity controlled compression ignition (RCCI): a pathway to controlled high-efficiency clean combustion, Int. J. Engine Res. 12 (2011) 209–226. https://doi.org/10.1177/1468087411401548.

[4] J. Benajes, A. Garcia, J. Monsalve-Serrano, V. Boronat, Achieving clean and efficient engine operation up to full load by combining optimized RCCI and dual-fuel diesel-gasoline combustion strategies, Energy Convers. Manag. 136 (2017) 142–151. https://doi.org/10.1016/j.enconman.2017.01.010.

[5] A. Paykani, A.-H. Kakaee, P. Rahnama, R.D. Reitz, Progress and recent trends in reactivity-controlled compression ignition engines, Int. J. Engine Res. 17 (2016) 481–524. https://doi.org/10.1177/1468087415593013.

[6] J. Li, W. Yang, D. Zhou, Review on the management of RCCI engines, Renew. Sustain. Energy Rev. 69 (2017) 65–79. https://doi.org/10.1016/j.rser.2016.11.159.

[7] R.D. Reitz, G. Duraisamy, Review of high efficiency and clean reactivity controlled compression ignition (RCCI) combustion in internal combustion engines, Prog. Energy Combust. Sci. 46 (2015) 12–71. https://doi.org/10.1016/j.pecs.2014.05.003.

[8] J. Benajes, A. García, J. Monsalve-Serrano, V. Boronat, Gaseous emissions and particle size distribution of dual-mode dual-fuel diesel-gasoline concept from low to full load, Appl. Therm. Eng. 120 (2017) 138–149. https://doi.org/10.1016/j.applthermaleng.2017.04.005.

[9] A. García, J. Monsalve-Serrano, D. Villalta, R. Lago Sari, Performance of a conventional diesel aftertreatment system used in a medium-duty multi-cylinder dual-mode dual-fuel engine, Energy Convers. Manag. 184 (2019) 327–337. https://doi.org/10.1016/j.enconman.2019.01.069.

[10] T. V. Johnson, Review of diesel emissions and control, Int. J. Engine Res. 10 (2009) 275–285. https://doi.org/10.1243/14680874JER04009.

[11] V. Praveena, M.L.J. Martin, A review on various after treatment techniques to reduce NOx emissions in a CI engine, J. Energy Inst. 91 (2018) 704–720. https://doi.org/10.1016/j.joei.2017.05.010.

[12] M.-F. Hsieh, J. Wang, Design and experimental validation of an extended Kalman filter-based NOx concentration estimator in selective catalytic reduction system applications, Control Eng. Pract. 19 (2011) 346–353. https://doi.org/10.1016/j.conengprac.2010.12.002.

[13] B. Pla, P. Bares, E. Sanchis, A. Aronis, Ammonia injection optimization for selective catalytic reduction aftertreatment systems, Int. J. Engine Res. (2020) 146808742093312. https://doi.org/10.1177/1468087420933125.

[14] J.K. Arora, M. Shahbakhti, Real-Time Closed-Loop Control of a Light-Duty RCCI Engine During Transient Operations, SAE Tech. Pap. (2017). https://doi.org/10.4271/2017-01-0767.Copyright.

[15] C. Guardiola, B. Pla, P. Bares, A. Barbier, Closed-loop control of a dual-fuel engine working with different combustion modes using in-cylinder pressure feedback, Int. J. Engine Res. (2019). https://doi.org/10.1177/1468087419835327.

[16] C. Jorques Moreno, O. Stenlaas, P. Tunestal, In-Cycle Closed-Loop Combustion Control for Pilot Misfire Compensation, in: SAE Tech. Pap., 2020: pp. 1–13. https://doi.org/10.4271/2020-01-2086.

[17] Y. Tan, W.H. Moase, C. Manzie, D. Nešić, I.M.Y. Mareels, Extremum seeking from 1922 to 2010, Proc. 29th Chinese Control Conf. CCC'10. (2010) 14–26.

[18] F. Zurbriggen, R. Hutter, C. Onder, Diesel-minimal combustion control of a natural gas-diesel engine, Energies. 9 (2016). https://doi.org/10.3390/en9010058.

[19] W. Wang, Y. Li, B. Hu, Real-time efficiency optimization of a cascade heat pump system via multivariable extremum seeking, Appl. Therm. Eng. 176 (2020) 115399. https://doi.org/10.1016/j.applthermaleng.2020.115399.

[20] S. Kumar, A. Mohammadi, D. Quintero, S. Rezazadeh, N. Gans, R.D. Gregg, Extremum Seeking Control for Model-Free Auto-Tuning of Powered Prosthetic Legs, IEEE Trans. Control Syst. Technol. 28 (2020) 2120–2135. https://doi.org/10.1109/TCST.2019.2928514.

[21] E. Hellstrom, D. Lee, L. Jiang, A.G. Stefanopoulou, H. Yilmaz, On-Board Calibration of Spark Timing by Extremum Seeking for Flex-Fuel Engines, IEEE Trans. Control Syst. Technol. 21 (2013) 2273–2279. https://doi.org/10.1109/TCST.2012.2236093.

[22] Y. Zhang, T. Shen, Cylinder pressure based combustion phase optimization and control in spark-ignited engines, Control Theory Technol. 15 (2017) 83–91. https://doi.org/DOI 10.1007/s12239−017−0092−7.

[23] R. Novella, B. Pla, P. Bares, P.J. Martinez-Hernandiz, Closed-Loop Combustion Control by Extremum Seeking with the Passive-Chamber Ignition Concept in SI Engines, in: SAE Tech. Pap., 2020: pp. 1–11. https://doi.org/10.4271/2020-01-1142.

[24] M. Lewander, A. Widd, B. Johansson, P. Tunestal, Steady state fuel consumption optimization through feedback control of estimated cylinder individual efficiency, 2012 Am. Control Conf. (2014) 4210–4214. https://doi.org/10.1109/acc.2012.6315075.

[25] R. van der Weijst, T. van Keulen, F. Willems, Constrained multivariable extremum-seeking for online fuel-efficiency optimization of Diesel engines, Control Eng. Pract. 87 (2019) 133–144. https://doi.org/10.1016/j.conengprac.2019.03.008.

[26] Q. Tan, P.S. Divekar, Y. Tan, X. Chen, M. Zheng, Pressure Sensor Data-Driven Optimization of Combustion Phase in a Diesel Engine, IEEE/ASME Trans. Mechatronics. 25 (2020) 694–704. https://doi.org/10.1109/TMECH.2020.2967874.

[27] M.F.J. Brunt, C.R. Pond, Evaluation of Techniques for Absolute Cylinder Pressure Correction, SAE Tech. Pap. (1997) SAE 970036. https://doi.org/10.4271/970036.

[28] M. Krstić, H.-H. Wang, Stability of extremum seeking feedback for general nonlinear dynamic systems, Automatica. 36 (2000) 595–601. https://doi.org/10.1016/S0005-1098(99)00183-1.

[29] D. Dochain, M. Perrier, M. Guay, Extremum seeking control and its application to process and reaction systems: A survey, Math. Comput. Simul. 82 (2011) 369–380. https://doi.org/10.1016/j.matcom.2010.10.022.

[30] K.T. Atta, M. Guay, Adaptive amplitude fast proportional integral phasor extremum seeking control for a class of nonlinear system, J. Process Control. 83 (2019) 147–154. https://doi.org/10.1016/j.jprocont.2018.10.006.

[31] D. Blanco-Rodriguez, Modelling and Observation of Exhaust Gas Concentrations for Diesel Engine Control, Springer International Publishing, Cham, 2014. https://doi.org/10.1007/978-3-319-06737-7.

[32] C.F. Aquino, Transient A/F Control Characteristics of the 5 Liter Central Fuel Injection Engine, in: SAE Tech. Pap. Ser., 1981. https://doi.org/10.4271/810494.

Contact Information

Contact details for the main author should be included here. Details may include mailing address, email address, and/or telephone number (whichever is deemed appropriate).

Acknowledgments

If the Acknowledgments section is not wanted, delete this heading and text.

Definitions/Abbreviations

BSFC	Brake specific fuel consumption
BSNOx	Brake specific engine-out NO_x emissions
CA50	Crank angle where 50% of the energy has been released
CAD	Crank angle degree
DI	Direct injection
EGR	Exhaust gas recirculation
ES	Extremum seeking
GF	Gasoline fraction
IMEP	Indicated mean effective pressure
LTC	Low temperature combustion
PFI	Port fuel injection
RCCI	Reactivity Controlled Compression Ignition
SOI	Start of injection
TDC	Top dead center